

Geodesic Motion of Neutral Particles around a Kerr-Newman Black Hole

Chen-Yu Liu,^{*} Da-Shin Lee,[†] and Chi-Yong Lin[‡]

Department of Physics, National Dong Hwa University, Hualien, Taiwan, R.O.C.

(Dated: November 15, 2017)

Abstract

We examine the dynamics of a neutral particle around a Kerr-Newman black hole, and in particular focus on the effects of the charge of the spinning black hole on the motion of the particle. We first consider the innermost stable circular orbits (ISCO) on the equatorial plane. It is found that the presence of the charge of the black hole leads to the effective potential of the particle with stronger repulsive effects as compared with the Kerr black hole. As a result, the radius of ISCO decreases as charge Q of the black hole increases for a fixed value of black hole's angular momentum a . We then consider a kick on the particle from its initial orbit out of the equatorial motion. The perturbed motion of the particle will eventually be bounded, or unbounded so that it escapes to spatial infinity. Even more, the particle will likely be captured by the black hole. Thus we analytically and numerically determine the parameter regions of the corresponding motions, in terms of the initial radius of the orbital motion and the strength of the kick. The comparison will be made with the motion of a neutral particle in the Kerr black hole.

PACS numbers: 04.70.-s 04.70.Bw 04.25.-g

^{*}Electronic address: ef850502@gmail.com

[†]Electronic address: dslee@mail.ndhu.edu.tw

[‡]Electronic address: lcyong@mail.ndhu.edu.tw

I. INTRODUCTION

The phenomena of accretion disks and jets formation will be the hallmark in observing the black hole [1, 2]. The energetic jets are created by the matter in accretion disks, and are powered perhaps from dynamic interactions within accretion disks or from processes associated with black holes. Relativistic jet formation may also explain observed gamma-ray bursts. Nevertheless, the matter particles in the surrounding of the black hole are significantly influenced by the gravitational pull. The investigation of the motion of particles near the black hole certainly is of great importance not only to explore the spacetime structure of the black hole, but also to find the appropriate mechanism for the formation of accretion disks and jets. In addition to the geodesic motion of test particles in ordinary general relativity, the interest of the subject has also gained attention in the field of higher dimensional gravity theories, more specifically in connection to braneworld models [3–5].

The dynamics of particles orbiting around the black hole has been extensively studied for Schwarzschild and Kerr black holes [1, 2, 6]. The exploration of the circular motion of the particle is also extended to Reissner-Nordström black holes [7, 8]. Recently, observational evidence for a correlation between jet power and black hole spin has been discovered [9]. This finding is consistent with numerical simulations, showing that powerful jets are generated by extracting energy from a spinning black hole together with the surrounding magnetic field [10]. These discoveries certainly motivated more investigations on the evolution of particles in weakly magnetized black holes. For example, in the presence of weak magnetic field, the motion of a charged particle near a Schwarzschild black hole is analyzed in [11–13], while around a Kerr black hole the charged particle can undergo chaotic motion [14–18]. Nevertheless, the Kerr-Newman metric represents a generalization of the Kerr metric, and describes spacetime in the exterior of a rotating charged black hole where, apart from gravitation fields, both electric and magnetic fields exist intrinsically from the black hole.

Although one might not expect that astrophysical black holes have a large residue electric charge, some accretion scenarios were proposed to investigate the possibility of the spinning charged black holes [19]. Thus, it is still of great interest to extend the previous studies to a Kerr-Newman black hole. The geodesic motion of a test particle in the Kerr-Newman spacetime have been investigated. In particular, in [20], a detailed analysis of the orbital circular motion of electrically neutral test particles on the equatorial plane of the Kerr-Newman

spacetime in the cases of black hole and naked singularity sources was presented. The types of geodesic motion also include spherical and nonspherical orbits of test charges [21], and possible capture of particles from plunge orbits by a black hole [22] (Also see [23] and references therein). The general features of the radial motion, and the motion of charge particles along the axis of symmetry and in the equatorial plane, or the special case of free-infalling particles were discussed in [24–26]. One way to explore the interplay between gravitational and electromagnetic fields of a Kerr-Newman black hole is to consider off-equatorial orbits of a charged particle near the black hole [27]. It is found that the stable off-equatorial orbits do not exist above the outer horizon of the black hole. The analytical solutions of the geodesic equations in the black hole spacetime were also found respectively in the Schwarzschild [28], Reissner-Nordström [29], and Kerr-Newman [30] black holes. In particular, the paper [30] provided a comprehensive classification of the orbits in radial and colatitudinal directions for a large variety of orbit configurations of the charge particle in a Kerr-Newman black hole. Additionally, the analytical solutions of geodesic motion for all types of orbits were presented in terms of elliptic functions dependent on the so-called Mino time [31]. According to these studies we can examine how the effects from electromagnetic fields intrinsically from the black hole affect the dynamics of the surrounding particles.

In this work, we will focus on the dynamics of a neutral particle orbiting around a Kerr-Newman black hole, mainly following the strategy developed by [14]. Most of results in [14] for a Kerr black hole will be generalized to a spinning charged black hole. The effects of electromagnetic fields associated with the Kerr-Newman black hole on a neutral particle are solely through the gravitational influence. Here we first consider the so-called innermost stable circular orbits (ISCO) of the particle on the equatorial plane ($\theta = \pi/2$). We explore, in particular, the effects of the black hole charge on the radius of ISCO via the appropriate effective potentials [20]. Afterwards, the particle, initially moving around some particular orbit, is perturbed by a kick along the θ direction. In this situation of possible astrophysical relevance, the kick could be given by another particles and/or photons. Then, the initial radius of the orbit and an amount of the kick form a two-dimensional parameter space. We provide an analytical analysis in the same fashion as [13] to identify the regions in the parameter space, that corresponds to the different asymptotic behaviors of the particle.

Although these trajectories can be described by means of the analytical solutions in the Mino time [30], here we would like to explore them in the proper time instead. The nontrivial

transformation between the Mino time and the proper time may suggest us to study the associated equations of motion directly in the proper time. Also in [30], in spite of the fact that all possible trajectories were discussed, however in this work, we mainly focus on the above-mentioned situation in more details. The effects of the charge of a spinning black hole on the final states of the kicked particle can be understood analytically later by studying the appropriate effective potential [13]. Finally, these analytical results will be reexamined by solving numerically the dynamical equations of the particle in the Kerr-Newman background with the corresponding initial conditions directly in the proper time. Same trajectories are believed to obtain as compared with the analytical solutions after the transformation from the Mino time to the proper time is carried out.

II. CIRCULAR MOTION OF A NEUTRAL PARTICLE AROUND KERR-NEWMAN BLACK HOLE

The spacetime outside a black hole with the gravitational mass M , charge Q , and angular momentum per unit mass $a = J/M$ is described by Kerr-Newman metric:

$$\begin{aligned} ds^2 &= g_{\mu\nu} dx^\mu dx^\nu \\ &= -\frac{(\Delta - a^2 \sin^2 \theta)}{\Sigma} dt^2 + \frac{a \sin^2 \theta (Q^2 - 2Mr)}{\Sigma} (dt d\phi + d\phi dt) \\ &\quad + \frac{\Sigma}{\Delta} dr^2 + \Sigma d\theta^2 + \frac{\sin^2 \theta}{\Sigma} ((r^2 + a^2)^2 - a^2 \Delta \sin^2 \theta) d\phi^2, \end{aligned} \quad (1)$$

where

$$\Sigma = r^2 + a^2 \cos^2 \theta, \quad \Delta = r^2 + a^2 + Q^2 - 2Mr. \quad (2)$$

The event horizon R_H can be found by solving $\Delta(r) = 0$, and is given by

$$R_H = M + \sqrt{M^2 - (Q^2 + a^2)} \quad (3)$$

with $M^2 > Q^2 + a^2$. Now we consider a test neutral particle with mass m moves in such a spacetime. Its Lagrangian is simply given by

$$L = -m \sqrt{-g_{\mu\nu} u^\mu u^\nu}, \quad (4)$$

where $u^\mu \equiv dx^\mu/d\tau$ is the four-velocity, and τ is proper time. Because the metric of Kerr-Newman black hole has no explicit t and ϕ dependence, they are cyclic coordinates in the

Lagrangian. The respective Killing vectors, $\xi_{(t)}^\mu$ and $\xi_{(\phi)}^\mu$, are given by

$$\xi_{(t)}^\mu = \delta_t^\mu, \quad \xi_{(\phi)}^\mu = \delta_\phi^\mu. \quad (5)$$

Then, the associated conserved quantities, namely energy and azimuthal angular momentum per unit mass, along a geodesic, can be constructed by the above Killing vectors as well as the four-momentum $p_\mu = mu_\mu$ of the particle:

$$\varepsilon = -p_\mu \xi_{(t)}^\mu / m, \quad \ell = p_\mu \xi_{(\phi)}^\mu / m. \quad (6)$$

Additionally, there exists a third constant of motion (the Carter constant), defined by [13]

$$\kappa = u_\mu u_\nu K^{\mu\nu} - (\ell - a\varepsilon)^2, \quad (7)$$

where

$$\begin{aligned} K^{\mu\nu} &= \Delta[k^\mu q^\nu - k^\nu q^\mu] + r^2 g^{\mu\nu}, \\ q^\mu &= \frac{1}{\Delta}[(r^2 + a^2)\delta_t^\mu + \Delta\delta_r^\mu + a\delta_\phi^\mu], \\ k^\mu &= \frac{1}{\Delta}[(r^2 + a^2)\delta_t^\mu - \Delta\delta_r^\mu + a\delta_\phi^\mu]. \end{aligned} \quad (8)$$

Using these three constants of motion and the normalization condition $u_\mu u^\mu = -1$, we are able to write down the equations of motion for the components of u^μ in terms of ε , ℓ , κ :

$$\dot{t} = \varepsilon - \frac{(Q^2 - 2Mr)((a^2 + r^2)\varepsilon - a\ell)}{\Delta\Sigma}, \quad (9)$$

$$\dot{\phi} = \frac{\ell}{\Sigma \sin^2 \theta} - \frac{a((Q^2 - 2Mr)\varepsilon + a\ell)}{\Delta\Sigma}, \quad (10)$$

$$\Sigma^2 \dot{r}^2 = [(r^2 + a^2)\varepsilon - a\ell]^2 - \Delta[r^2 + \kappa + (\ell - a\varepsilon)^2], \quad (11)$$

$$\Sigma^2 \dot{\theta}^2 = \kappa + (\ell - a\varepsilon)^2 - a^2 \cos^2 \theta - \left(a\varepsilon \sin \theta - \frac{\ell}{\sin \theta} \right)^2. \quad (12)$$

The over dot means the derivative with respect to the proper time τ .

We restrict the particle to move on the equatorial plane of the black hole by choosing $\theta = \pi/2$, and $\dot{\theta} = 0$ so that $\kappa = 0$ from (12). The equation of the motion along the radial direction in (11) thus becomes

$$\Sigma^2 \dot{r}^2 = r^4 \varepsilon^2 + 2a\ell\varepsilon(Q^2 - 2Mr) + a^2(\varepsilon^2(r^2 + 2Mr - Q^2) - r^2) - (\Delta - a^2)(r^2 + \ell^2). \quad (13)$$

The equation (13) allows us to define the effective potential V_{eff} by requiring

$$\frac{1}{2}\dot{r}^2 + V_{\text{eff}}(r, \alpha) = \frac{\varepsilon^2 - 1}{2}, \quad (14)$$

where α denotes a collection of the parameters of the Kerr-Newman black hole and the test neutral particle, namely $\alpha = (M, Q, a, \varepsilon, \ell)$

$$V_{\text{eff}}(r, \alpha) = -\frac{M}{r} + \frac{\ell^2 + (1 - \varepsilon^2)a^2 + Q^2}{2r^2} - \frac{M(\ell - a\varepsilon)^2}{r^3} + \frac{Q^2(\ell - a\varepsilon)^2}{r^4}. \quad (15)$$

In the limits of $Q = 0$ and $Q = 0$, $a = 0$, the effective potential reduces to the ones for the Kerr and Schwarzschild black holes respectively [1, 2]. There are several distinct classes of motion, depending on whether the black hole spin and azimuthal angular momentum of the particle are aligned $\ell a > 0$ or oppositely aligned $\ell a < 0$. Without losing generality, we keep ℓ positive and choose a to be either positive or negative. In the Kerr-Newman black hole, the effective potential has the Q^2 dependence, and thus the sign of Q will not be relevant. Thus we choose $Q > 0$ in the present work. The non-zero charge of the black hole seems to give repulsive effects to the particle as seen from its contributions to the centrifugal potential of the $1/r^2$ term as well as the relativistic correction of the $1/r^4$ term. These repulsive effects will shift the radius of the stable circular motion toward the black hole, as will be shown later. Also, the value of the ε certainly determines whether or not the particle has chance to escape from the black hole to spatial infinity.

To determine the circular motion, one may define $R(r)$ by the right hand side of the equation (13),

$$R(r) = r^4\varepsilon^2 + 2a\ell\varepsilon(Q^2 - 2Mr) + a^2(\varepsilon^2(r^2 + 2Mr - Q^2) - r^2) - (r^2 + Q^2 - 2Mr)(r^2 + \ell^2). \quad (16)$$

Thus its zero tells us the radius, say r_o , at which the velocity along the r direction vanishes. The existence of the circular orbits requires that the first derivative of R with respect to r at $r = r_o$ vanishes. This means zero-acceleration along the r direction. Moreover the condition $R''(r_o) \geq 0$ guarantees that circular motion is stable. The first two conditions give:

$$r^4\varepsilon^2 + 2a\ell\varepsilon(Q^2 - 2Mr) + a^2(\varepsilon^2(r^2 + 2Mr - Q^2) - r^2) - (r^2 + Q^2 - 2Mr)(r^2 + \ell^2) = 0, \quad (17)$$

$$r[(3Mr - Q^2) + 2r^2(\varepsilon^2 - 1)] + \ell((M - r)\ell - 2aM\varepsilon) + a^2(M\varepsilon^2 + r(\varepsilon^2 - 1)) = 0, \quad (18)$$

from which, ε_o and ℓ_o for this circular orbit with a given radius r_o are determined straightforwardly as

$$\varepsilon_o = \frac{a\sqrt{Mr_o - Q^2} + (Q^2 + r_o^2 - 2Mr_o)}{r_o\sqrt{2Q^2 + r_o^2 - 3Mr_o + 2a(Mr_o - Q^2)^{1/2}}}, \quad (19)$$

$$\ell_o = \frac{a(Q^2 - 2Mr_o) + (a^2 + r_o^2)\sqrt{Mr_o - Q^2}}{r_o\sqrt{2Q^2 + r_o^2 - 3Mr_o + 2a(Mr_o - Q^2)^{1/2}}}. \quad (20)$$

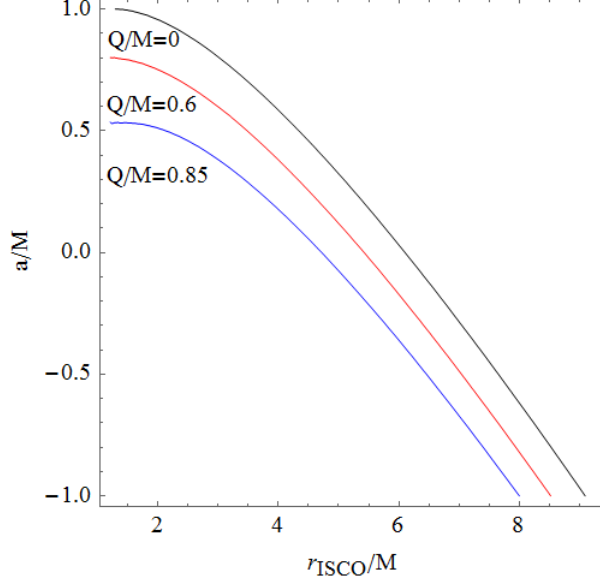


FIG. 1: The dependence of the radius r_{ISCO} on black hole's angular momentum per unit mass a and charge per unit mass Q .

That is, we must choose ε_o and ℓ_o given the equations above in order for a neutral particle to take a circular orbit of radius r_o around the Kerr-Newman black hole. Apparently, r_o can not be arbitrarily small. When the radius r_o is smaller than the so-called the radius of the inner most stable circular orbit, r_{ISCO} given by $R''(r_o) = 0$, the circular motion becomes unstable [5, 20]. Thus r_{ISCO} satisfies

$$(6 r_{\text{ISCO}}^2 + a^2)(\varepsilon_o^2 - 1) + 6Mr_{\text{ISCO}} - \ell_o^2 - Q^2 = 0. \quad (21)$$

Substituting the expressions (19) and (20) into (21) we arrive at the following polynomial equation for the radius of the circular orbits, also obtained in [3],

$$Mr_{\text{ISCO}}(6Mr_{\text{ISCO}} - r_{\text{ISCO}}^2 - 9Q^2 + 3a^2) + 4Q^2(Q^2 - a^2) - 8a(Mr_{\text{ISCO}} - Q^2)^{3/2} = 0. \quad (22)$$

In Fig. 1 we plot the behavior of r_{ISCO} for various combinations of parameters a and Q .

For a given Q , in the case of $a > 0$ the radius of the ISCO decreases with the increase of a whereas the radius for $a < 0$ increases when the absolute value of a increases. In particular, we highlight the following three cases for the neutral black hole, $Q = 0$. (A) if the black hole does not rotate, i.e., Schwarzschild black hole ($a = 0$), we have $r_{\text{ISCO}} = 6M$, while (B) in extreme limit $a = 1$, we find $r_{\text{ISCO}} = 1M$ when the particle rotates in the same orientation as the Kerr black hole, but (C) $r_{\text{ISCO}} = 9M$ in the opposite orientation. For a nonzero Q ,

the ISCO radius generally is smaller than in the $Q = 0$ case for a given a . This results from the fact that the charge of the black hole seems to give more repulsive effects on the particle as compared with the $Q = 0$ case, as seen in the effective potential (15). In comparison with (A), when $Q = M, a = 0$, the ISCO radius is $r_{\text{ISCO}} = 1M$. All circular motion corresponds to its energy $\varepsilon < 1$ [20]. In the next section, we will explore the case that the particle, which initially orbits on the equatorial plane, experiences an impulse force in the direction normal to the plane.

III. FINAL STATES OF THE PARTICLE KICKED OFF FROM AN INITIAL CIRCULAR MOTION

In general, the coupled equations of motion for a neutral particle moving around a Kerr-Newman black hole are too complicated to solve in the proper time. In order to make analytic investigation possible, we consider a special case that the particle is knocked out of its original circular motion on the equatorial plane by an impulse force along the θ direction. Thus the circular motion of the particle and the influence of the kick can be effectively summarized by the four-velocity at the moment when the force acts on the particle,

$$u_{i\nu} = (-\varepsilon, 0, r_o^2 \dot{\theta}_k, \ell_o). \quad (23)$$

The radius r_o and the strength of the kick, $\dot{\theta}_k$ are two initial parameters, from which the evolution of the particle follows. Later, we will provide a complete analysis to determine the type of the final states for various choices of r_o and $\dot{\theta}_k$. Since the kick is along the θ direction, the particle's azimuthal angular momentum remains the same value as ℓ_o in (20). The energy ε on the other hand will be modified after a kick and the normalization condition for the $u_{i\nu}$ gives

$$\varepsilon = \frac{\ell_o a (2Mr_o - Q^2) + r_o \Delta_o^{1/2} \sqrt{(r_o^4 + a^2(r_o^2 + 2Mr_o - Q^2))(1 + r_o^2 \dot{\theta}_k^2) + r_o^2 \ell_o^2}}{r_o^4 + a^2(r_o^2 + 2Mr_o - Q^2)}, \quad (24)$$

where, $\Delta_o \equiv \Delta(r_o)$. The form of ε is chosen so that the four-velocity is future-directed. In addition, the Carter constant reduces to

$$\kappa = r_o^4 \dot{\theta}_k^2 \quad (25)$$

in (12).

The effective potential defined in (15) depends on both the azimuthal angular momentum ℓ and the energy ε . So, the analysis of the particle's dynamics proceeds by rewriting (13) as

$$\Sigma^2 \dot{r}^2 = (r^4 + a^2(r^2 + 2Mr - Q^2))(\varepsilon - V_+)(\varepsilon - V_-) \quad (26)$$

where

$$V_{\pm}(r) = \frac{\ell a(2Mr - Q^2) \pm \Delta^{1/2} \sqrt{a^2(\kappa + r^2)(r^2 + 2Mr - Q^2) + r^4(\kappa + r^2 + \ell^2)}}{r^4 + a^2(r^2 + 2Mr - Q^2)}. \quad (27)$$

The acceleration $\ddot{r}(r)$ can be obtained by taking the proper time derivative of (26), and we find

$$\ddot{r}(r) = -\frac{r^4 + a^2(r^2 + 2Mr - Q^2)}{2r^4}(\varepsilon - V_-(r))V'_+(r). \quad (28)$$

Eq. (28) shows that when $\varepsilon > V_-(r_o)$, $\ddot{r}(r_o) \propto -V'_+(r_o)$, where r_o is the initial radius of the orbital motion. Thus, $V_+(r)$ is more relevant for the dynamics of the particle. Apparently, whether the particle potentially moves toward the spatial infinity or is captured by the black hole crucially depends on the sign of $\ddot{r}(r_o)$. The curve of the critical $\dot{\theta}$ that separates the two cases in the parameter space is determined by

$$V'_+(r_o, \dot{\theta}_c) = 0. \quad (29)$$

The behavior is illustrated in Fig. 2 for a critical kick of $\dot{\theta}_c$. The region to the left of the critical curve corresponds to $\ddot{r} < 0$ while the other side corresponds to $\ddot{r} > 0$. The critical kick of $|\dot{\theta}_c|$ starts from zero at $r_o = r_I$ and approaches to infinity as r_o approaches r_F . For a given a and Q , r_I and r_F satisfy

$$a \sqrt{Mr_I - Q^2} [r_I^2(2Q^2 + r_I(2r_I - 3M)) + a^2(Q^2 + r_I(2r_I - M))] + r^4(a^2 + 2Q^2 + r_I(r_I - 3M)) + a^4(Mr - Q^2) = 0, \quad (30)$$

$$a^2(r_F + M) + r_F(2Q^2 + r_F(r_F - 3M)) = 0. \quad (31)$$

Thus, the values of r_I and r_F decrease as the value of Q (and/or a) increases as shown in Fig. 3, and they coincide when $a = 0$ for any possible Q , also seen in the figure. These are the generalization of the findings in [14] to the Kerr-Newman black hole. In Fig. 3, the r_{ISCO} is also shown for various choices of a and Q . With an initial $r_o > r_{\text{ISCO}}$ and a given value of $\dot{\theta}_k$ of a kick, one can determine the possible sign of \ddot{r} from Fig. 2. Nevertheless, for $r_{lc} < r_o < r_{\text{ISCO}}$ where $R''(r_o) < 0$, the particle can be initially in unstable circular motion.

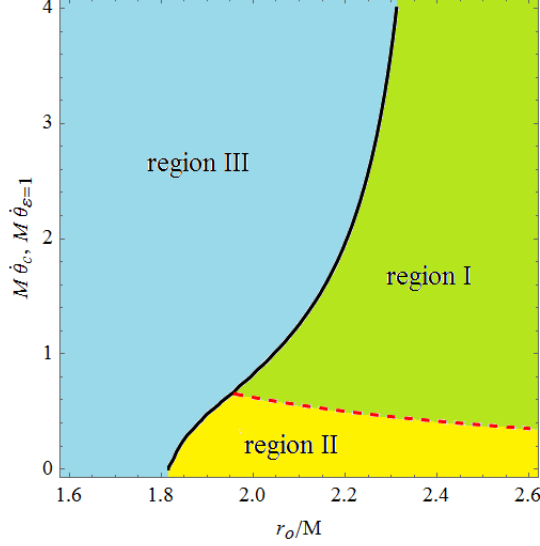


FIG. 2: The solid curve of θ_c that corresponds to $V'_+(r_o, \dot{\theta}_c) = 0$ is plotted with respect to r_o for $a = 0.96M$ and $Q = 0.2M$. $|\dot{\theta}_c|$ starts from zero at $r_o = r_I = 1.82M$ and approaches to infinity as r_o approaches $r_F = 2.43M$. The red dashed curve describes $|\dot{\theta}_{\varepsilon=1}|$ when the energy of a particle is $\varepsilon = 1$.

The radius of the last circular orbit r_{lc} , at which both ε_o in (19) and ℓ_o in (20) become infinity, is found by

$$2a(Mr_{lc} - Q^2)^{1/2} + 2Q^2 + r_{lc}(r_{lc} - 3M) = 0 \quad (32)$$

and is shown in Fig. 2 for comparison. When $\ddot{r} > 0$, the particle may escape to spatial infinity or be bounded, depending on whether its energy ε is greater than one or not. On the other hand, for $\ddot{r} < 0$, the particle is mainly captured by the black hole. Thus, we will consider these cases separately below. As for negative value of a for the counter-rotation motion for the particle around a Kerr-Newman black hole, since $V_{\pm}(-a) = -V_{\mp}(a)$ in (27), the same strategy for $a > 0$ case can be straightforwardly applied [4].

In the regime of the parameters $(\dot{\theta}_k, r_o)$ with $\ddot{r} > 0$, the important criterion to determine whether the particle will escape to spatial infinity or stay in the bounded motion is set by the condition $\varepsilon = 1$ in (24). The corresponding value of the kick $\dot{\theta}_{\varepsilon=1}$ is obtained by

$$|\dot{\theta}_{\varepsilon=1}| = \left[\frac{(Q^2 - 2Mr_o)(a^2 + r_o^2 - 2a\ell_o) + (\Delta_o - a^2)\ell_o^2}{r_o^4 \Delta} \right]^{1/2}, \quad (33)$$

and shown in Fig. 2. Inside regime (I) in Fig. 2, since the impulse force is adequately strong or the orbital radius is sufficiently large, the particle then has large enough energy

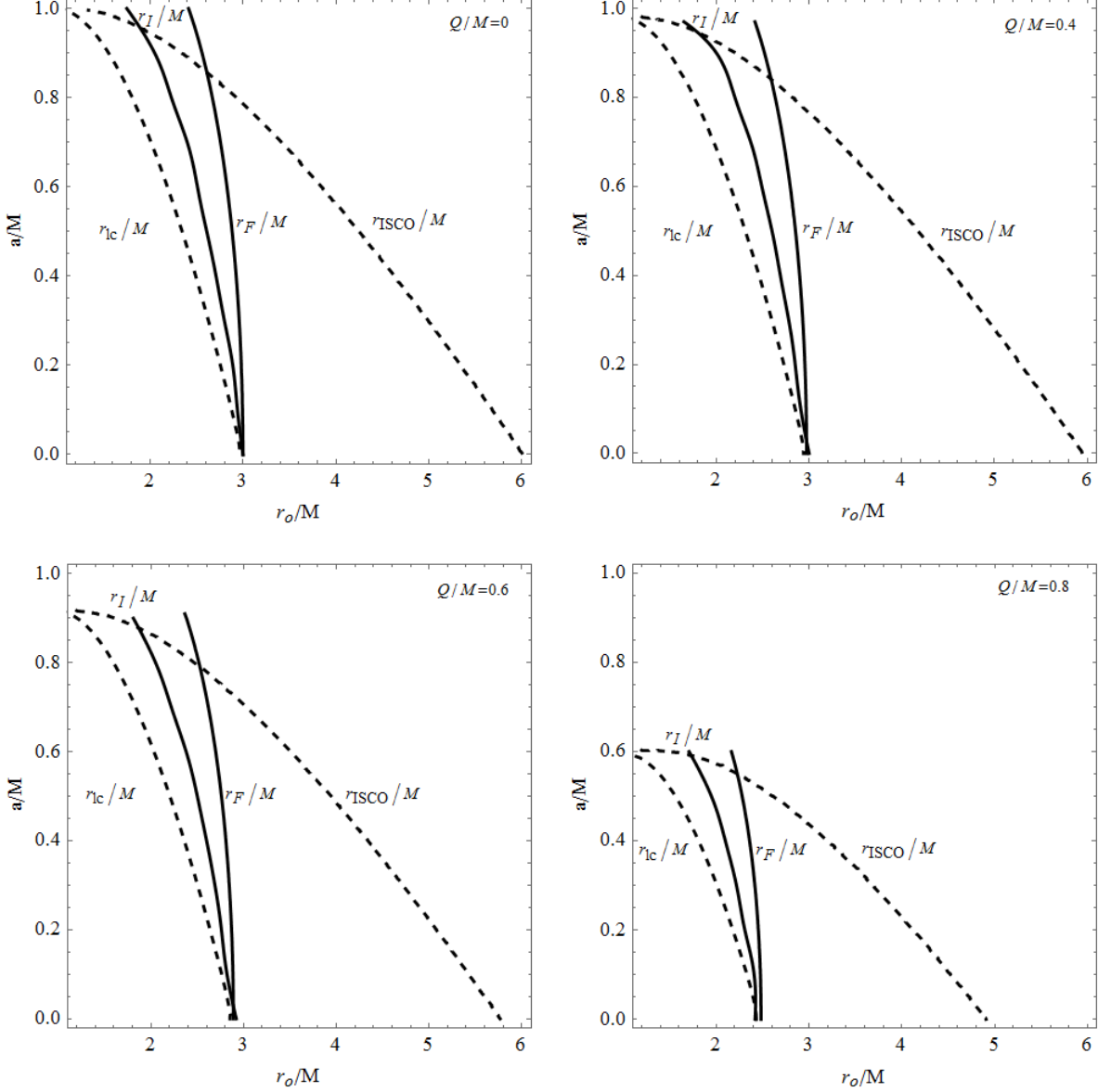


FIG. 3: The dependence of r_I and r_F on a and Q is shown. Also, r_{lc} and r_{ISCO} are displayed as the function of a and Q for comparison. When $r_o > r_{ISCO}$, the stable initial circular motion exists, and when $r_{lc} < r_o < r_{ISCO}$, the unstable circular motion is possible.

to escape from the black hole to spatial infinity. This behavior can also be understood from the potential energy V_+ in Fig. 4a (regime (I)). However, in the regime (II) $\varepsilon < 1$, the corresponding energy potential shows that the particle still get trapped around the local minimum of the effective potential (Fig. 4b), and remains the bounded motion with slightly larger radius as compared with the initial radius [4]. On the contrary, for $(\dot{\theta}_k, r_o)$ corresponding to an initial circular motion in the regime (III), the particle with $\ddot{r} < 0$ will

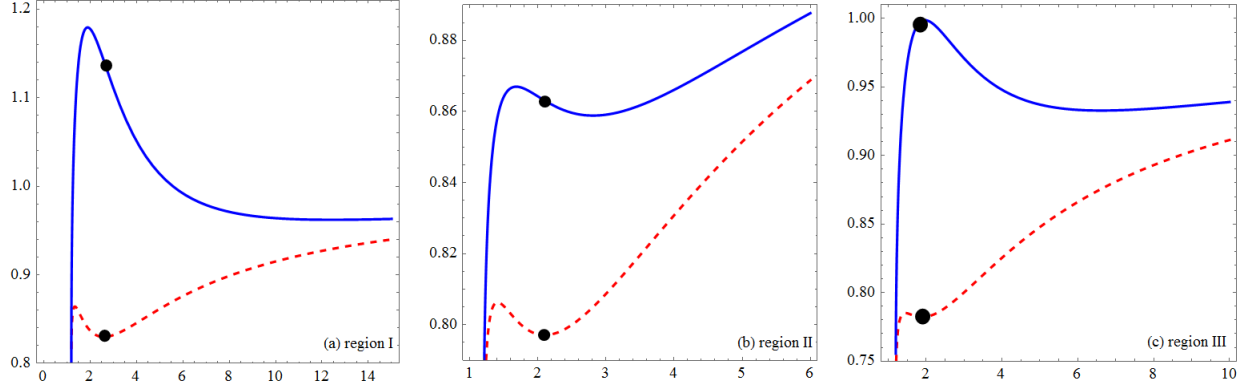


FIG. 4: Illustrations of $V_+(r)$ for a particle in the black hole geometry of $a = 0.96M$ and $Q = 0.2M$ before (dashed red line) and after (solid blue line) a kick with the initial parameters in the regime (I) (a): $r_o = 2.6M, \dot{\theta}_k = 0.5/M$; $\ddot{r} > 0, \varepsilon > 1$, (II) (b): $r_o = 2.1M, \dot{\theta}_k = 0.3/M$; $\ddot{r} > 0, \varepsilon < 1$, and (III) (c): $r_o = 1.9M, \dot{\theta}_k = 0.7/M$; $\ddot{r} < 0$. The black dots on the dashed red line and the solid blue line indicate the respective position of the test particle before and right after the kicks.

move toward the black hole, and finally gets captured. This evolution is also seen by the potential energy (Fig. 4c) in the regime (III). All these behaviors will be finally justified by numerically solving the equations of motion of the particle.

IV. TRAJECTORIES OF THE PARTICLE FROM SOLVING ITS DYNAMICAL EQUATIONS IN THE KERR-NEWMAN BLACK HOLE

The dynamics of a neutral particle of mass m in curved spacetime is governed by the geodesic equation

$$mu^\nu \nabla_\nu u^\mu = 0. \quad (34)$$

In the Kerr-Newman black hole geometry, the equations of motion of the particle for the radial and polar components are

$$\ddot{r} = (\Delta r \dot{\theta}^2 + a^2 \sin^2 \theta \dot{r} \dot{\theta}) / \Sigma + [XY(aZ \sin^2 \theta - \frac{Y}{4}) + GZ^2 \sin^4 \theta] / \Delta \Sigma^5, \quad (35)$$

$$\ddot{\theta} = (a^2 \sin^2 \theta (\Delta \dot{\theta} - \dot{r}^2) - 4\Delta r \dot{r} \dot{\theta}) / 2\Sigma\Delta + [JY + HZ^2 \cos \theta \sin^5 \theta + \frac{a^2 \sin^2 \theta Y^2}{8}(Q^2 + 2Mr)] / \Delta \Sigma^5 \quad (36)$$

accompanied with two conserved quantities, ε (24) and ℓ_o (20), to be determined by the initial radius of the orbit r_o and a kick θ_k . Here X, Y, Z, P, G, J, H are shorthand notations

for

$$\begin{aligned}
X &= r(Q^2 + Mr) - a^2 M \cos^2 \theta, \\
Y &= 2a\ell(Q^2 - 2Mr) + a^4 \varepsilon + 2r^4 \varepsilon + a^2 \varepsilon(2Mr + 3r^2 - Q^2) + a^2 \Delta \varepsilon \cos 2\theta, \\
Z &= a(a\ell + \varepsilon(Q^2 - 2Mr)) - \ell \Delta / \sin^2 \theta, \\
P &= r(a^2 + Q^2 - Mr) + a^2(M - r) \cos^2 \theta, \\
G &= a^4(M - r) \cos^2 \theta + r(a^2(a^2 + Q^2 - Mr) + 2a^2)(a^2 + r^2) \cos^2 \theta / \sin^2 \theta + (r^4 - a^4) / \sin^2 \theta, \\
J &= 16a(a^2 + r^2)(Q^2 - 2Mr) \cos \theta / \sin \theta \\
&\quad \times (2\ell(\Delta - a^2) + a^2 \ell - a\varepsilon(Q^2 - 2Mr) + a \cos(2\theta)(a\ell + \varepsilon(Q^2 - 2Mr))), \\
H &= -a^4 \Delta + r^2(a^2 + r^2)^2 / \sin^4 \theta + a^2(a^4 - r^2(-4Mr + 2Q^2 + r^2)) / \sin^2 \theta \\
&\quad + (a^2(a^2 + r^2)^2 / \sin^2 \theta - 2a^4 \Delta) \cos^2 \theta / \sin^2 \theta.
\end{aligned} \tag{37}$$

We then solve (35) and (36) numerically for a neutral particle around the black hole ($a/M = 0.9$, $Q/M = 0.2$) directly in the proper time. For the parameters in the regime I, with $\ddot{r} > 0$ and the energy $\varepsilon > 1$, the effective potential Fig. 4a shows that the particle of sufficiently large energy can escape to spatial infinity with a trajectory in Fig. 5a. As for the parameters in the regime II, since the kick does not give the particle sufficient energy ($\varepsilon < 1$, $\ddot{r} > 0$), the particle remains the bounded motion as seen from the effective potential in Fig. 4b with a trajectory in Fig. 5b. However, in the regime of the parameters III, the corresponding effective potential is shown in Fig. 4c with acceleration toward the black hole. Thus, the particle finally falls into the black hole in a trajectory in Fig. 5c.

An extensive numerical study is employed with the method of basin of attraction. The idea of basin of attraction is to identify the sets of initial values, from which the dynamical system tends to asymptotically evolve into an attractor. As to astrophysical observations of interest, we will restrict the initial conditions with the energy $\varepsilon > 1$, so that the particle may either get captured by the black hole, or escape to spatial infinity.

The plot of basin of attraction for the black hole $Q/M = 0.1$ and $a/M = 0.9$ is shown in Fig. 6 with the initial radius of the orbit motion and the energy after a kick in the regions $r_{lc} = 1.54M < r_o < 7M$, and $1 < \varepsilon < 1.24$. Notice that the radius of the inner most stable circular motion, the last circular motion (32), and the black hole horizon are $r_{ISCO} = 2.29M$, $r_{lc} = 1.54M$, and $r_H = 1.42M$ for reference. The maxima integration time is about $\tau = 10^4 M$. The particle is captured by the black hole with initial conditions lying

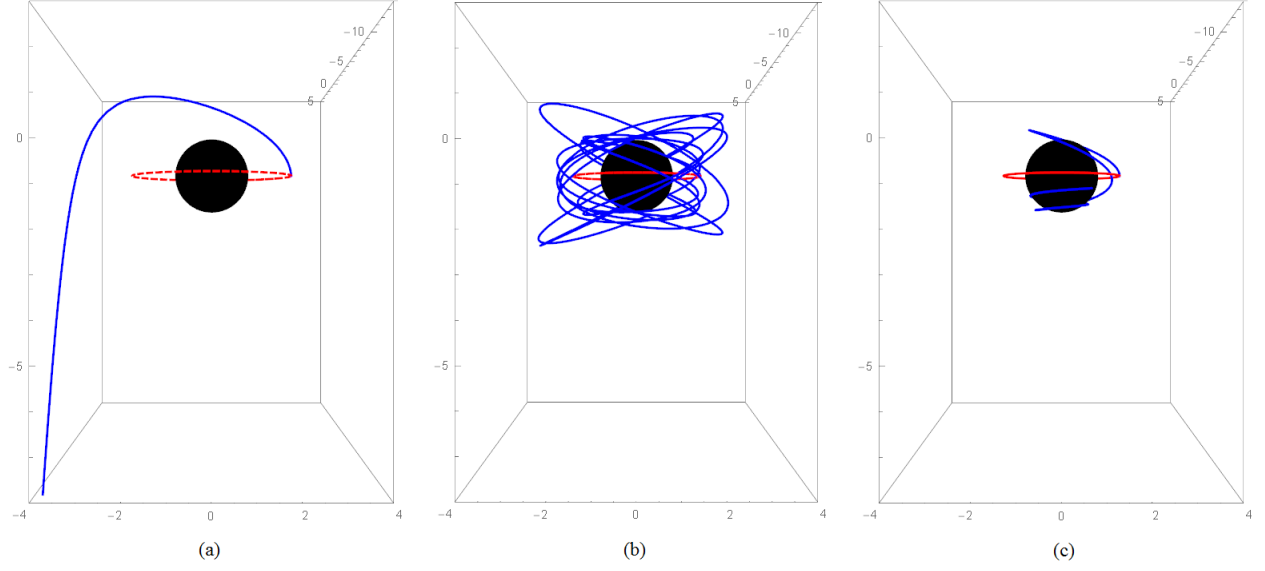


FIG. 5: Demonstrations of trajectories for a particle in the black hole geometry of $a = 0.96M$ and $Q = 0.2M$ with the same parameters as in (4) in the regime (I) (a): $r_o = 2.6M, \dot{\theta}_k = 0.5/M$; $\ddot{r} > 0, \varepsilon > 1$, (II) (b): $r_o = 2.1M, \dot{\theta}_k = 0.3/M$; $\ddot{r} > 0, \varepsilon < 1$, and (III) (c): $r_o = 1.9M, \dot{\theta}_k = 0.7/M$; $\ddot{r} < 0$. The black region represents interior of the horizon, and the circle (red) means the initial orbit of the particle.

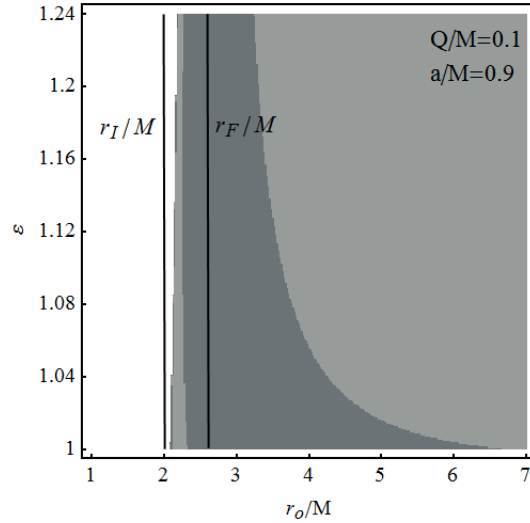


FIG. 6: The basin of attraction plot for a neutral particle when $Q/M = 0.1$ and $a/M = 0.9$. r_I and r_F are shown as well. See the text for detailed descriptions on the shaded (blank) zones in parameter space (r_o, ε) .

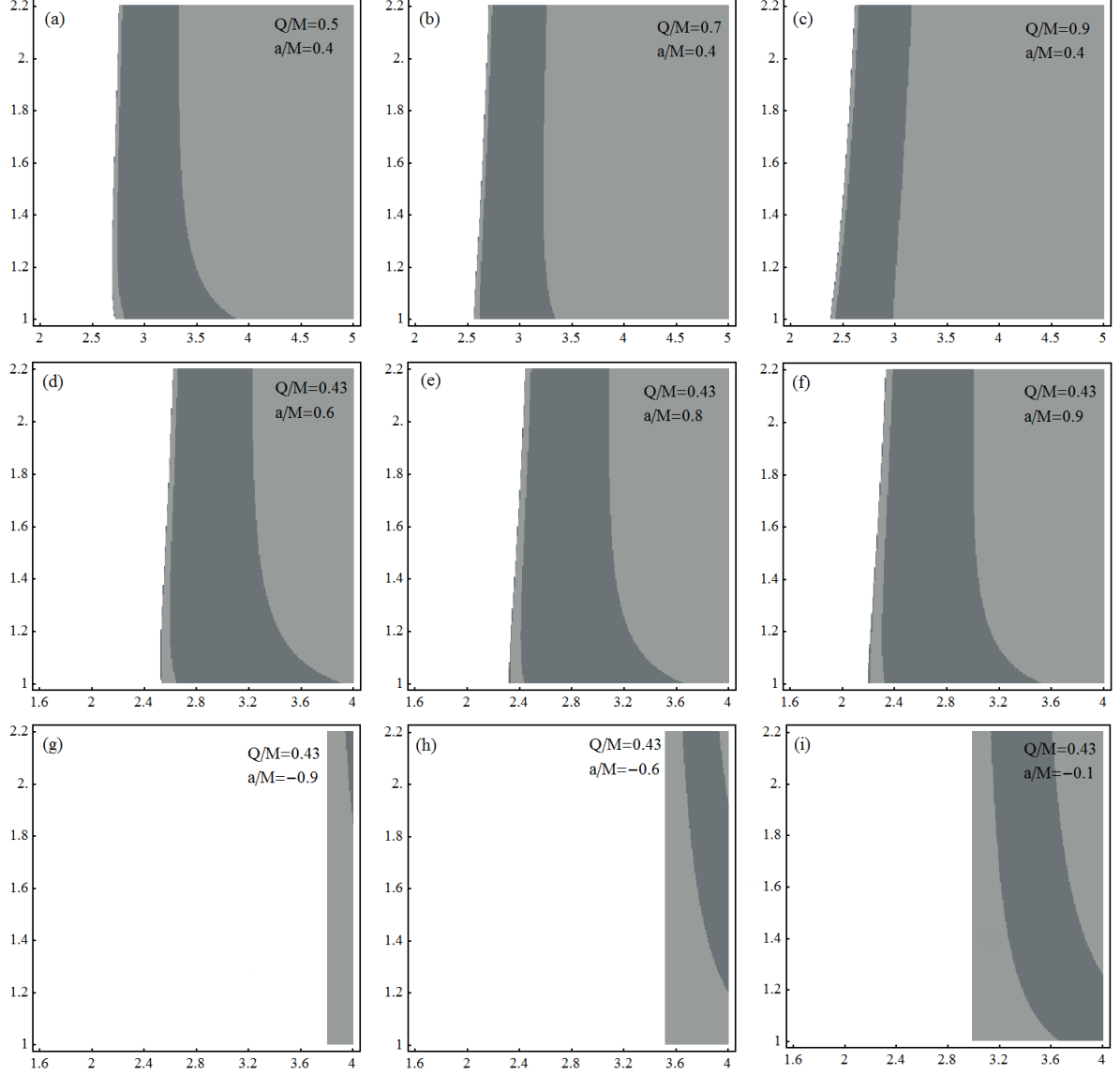


FIG. 7: The basin of attraction plot for a neutral particle in parameter space (r_o, ε) as in Fig. (6), when (a) : $Q/M = 0.5$, (b) : $Q/M = 0.7$, (c) $Q/M = 0.9$ for a fixed $a/M = 0.4$; and (d) : $a/M = 0.6$, (e) : $a/M = 0.8$, (f) : $a/M = 0.9$, (g) : $a/M = -0.9$, (h) : $a/M = -0.6$, (i) : $a/M = -0.1$ for a fixed $Q/M = 0.43$.

in the blank area, and escape to spatial infinity in the grey area. In particular, the direction of the escape is opposite to (same as) the initial kick with the (r_o, ε) in the light(dark) grey area. The radius of $r_I = 2.03M$ and $r_F = 2.55M$ in (30) are also plotted. For $\varepsilon > 1$, the particle will fall into the black hole for $r_o < r_I$, and escape to spatial infinity for $r_o > r_F$ as seen in the graph. The result of [13] can be reproduced in the $Q = 0$ case. In Fig. 7a-7c,

the blank area of (r_0, ε) to the capture decreases as the value of Q increases because the increase of Q will lead to larger repulsive effects to the dynamics of the particle as also seen in (15). Along the same line of thoughts, the capture region in Fig. 7d-7f increases as a ($a > 0$, for co-rotation) decreases or the absolute value of a ($a < 0$, for counter-rotation) increases, also seen in Fig. 7g-7i. Moreover, numerical calculation indicates that the basin boundaries are regular lines, as predicted by the analytical results in (33). They should be the regular motion with no chaotic behavior. Thus, the chaoticness of the motion might be seen when the particle under consideration carries a charge with the inclusion of the magnetic fields [13], which deserves further study.

V. SUMMARY AND OUTLOOK

In summary, the dynamics of a neutral particle around a Kerr-Newman black hole is studied with emphasis on how the electromagnetic fields intrinsically generated from the spinning charged black hole influences the particle's dynamics. We first examine the innermost stable circular orbits on the equatorial plane. It is found that the presence of the charge of the black hole gives the effective potential of the particle with stronger repulsive effects as compared with the Kerr black hole. As a result, the radius of ISCO decreases as the value of Q increases for a fixed angular momentum of the black hole a . We consider an impulse that kicks the particle which initially moves around an orbit, out of the equatorial plane. After a kick, the particle may remain the bounded motion, escape to spatial infinity, or fall into the black hole. We then provide the analytical and numerical studies to identify the regions in the parameter space which lead to the above respective final states. In particular, when the particle is captured by the black hole, the corresponding region in the parameter space decreases as Q increases. Additionally, the boundary of the parameters $(\dot{\theta}_k, r_o)$ between the capture and runaway regions appears as a regular curve. The chaotic motion thus may be expectedly seen for the motion of a charged particle in the external magnetic field [13]. Our work certainly provides the first step toward understanding the dynamics of the particle moving in the spacetime that has a spinning charged black hole. In the next step we will consider the motion of the charged particle to explore its chaotic behavior in the Kerr-Newman black hole with and/or without an external magnetic field. It would be of great interest to compare with the chaotic phenomena of a charged particle

in the magnetized Kerr black hole.

Acknowledgments

This work was supported in part by the Ministry of Science and Technology, Taiwan.

-
- [1] C. W. Misner, K. S. Thorne, and J. A. Wheeler, *Gravitation* (W. H. Freeman and Company, San Francisco, 1973).
 - [2] J. B. Hartle, *Gravity: An Introduction to Einstein's General Relativity* (Addison-Wesley, 2003).
 - [3] A. N. Aliev and A. E. Gumrukcuoglu, Phys. Rev. D **71**, 104027 (2005).
 - [4] Z. Stuchlik and A. Kotrlova, Gen. Rel. Grav. **41**, 1305 (2009).
 - [5] M. Blaschke and Z. Stuchlk, Phys. Rev. D **94**, no. 8, 086006 (2016).
 - [6] D. Pugliese, H. Quevedo and R. Ruffini, Phys. Rev. D **84**, 044030 (2011).
 - [7] D. Pugliese, H. Quevado, and R. Ruffini, Phys. Rev. D **83**, 024021 (2011).
 - [8] D. Pugliese, H. Quevado, and R. Ruffini, Phys. Rev. D **83**, 104052 (2011).
 - [9] R. Narayan and J. McClintock, Mon. Not. R. Astron. Soc. **419**, L69 (2012).
 - [10] A. Tchekhovskoy, R. Narayan and J. C. McKinney, Mon. Not. Roy. Astron. Soc. **418**, L79 (2011).
 - [11] V. P. Frolov and A. A. Shoom, Phys. Rev. D **82**, 084034 (2010).
 - [12] V. P. Frolov, Phys. Rev. D **85**, 024020 (2012).
 - [13] M. Al Zahrani, Valeri P. Frolov and Andrey A. Shoom, Phys. Rev. D. **87**, 084043 (2013).
 - [14] A. M. Al Zahrani. Phys. Rev. D **90**, 044012 (2014).
 - [15] R. Shiose, M. Kimura, and T. Chiba, Phys. Rev. D **90**, 124016 (2014).
 - [16] Y. Nakamura and T. Ishizuka, Astrophys. Space Sci. **210**, 105 (1993).
 - [17] M. Takahashi and H. Koyama, Astrophys. J. **693**, 472 (2009).
 - [18] S. Hussain, I. J. M. Hussain, Eur. Phys. J. C **74**, 3210 (2014).
 - [19] T. Damour, R. Hanni, R. Ruffini, and J. Wilson, Phys. Rev. D **17**, 1518 (1978).
 - [20] D. Pugliese, H. Quevedo and R. Ruffini, Phys. Rev. D **88**, 024042 (2013).
 - [21] M. Johnston and R. Ruffini, Phys. Rev. D, **10**, 2324 (1974).
 - [22] P. J. Young, Phys. Rev. D **14**, **3281** (1976).

- [23] N. A. Sharp, Gen. Relativ. Gravit. 10, **659** (1979).
- [24] J. Bicak, Z. Stuchlik, and V. Balek, Bull. Astron. Inst. Czech. **40**, 65 (1989).
- [25] V. Balek, J. Bicak, and Z. Stuchlik, Bull. Astron. Inst. Czech. **40**, 133 (1989).
- [26] Z. Stuchlik, J. Bicak, and V. Balek, Gen. Relativ. Gravit. **31**, 53 (1999).
- [27] J. Kovar, Z. Stuchlik, and V. Karas, Classical Quantum Gravity 25, 095011 (2008).
- [28] Y. Hagihara, Jpn. J. Astron. Geophys. **8**, 67 (1931).
- [29] S. Grunau and V. Kagramanova, Phys. Rev. D **83**, 044009 (2011).
- [30] E. Hackmann and H. Xu, Phys. Rev. D **87**, 124030 (2013).
- [31] Y. Mino, Phys. Rev. D **67**, 084027 (2003).